ABUNDANCE AND SIZE DISTRIBUTION OF INCLUSIONS IN CV3 CHONDRITES BY X-RAY IMAGE ANALYSIS. D. S. Ebel[1,4], K. Leftwich[2,5], C. E. Brunner[2,6], and M. K. Weisberg[1,3,7]. [1]Department of Earth and Planetary Sciences, American Museum of Natural History, Central Park West at 79th St., New York, NY 10024, [2]Western Kentucky University, 1906 College Heights Blvd., Bowling Green, KY 42101. [3]Dept. of Physical Sciences, Kingsborough College, City University of New York, Brooklyn, NY 11235. [4](debel@amnh.org), [5](kristin.leftwich@wku.edu), [6](chelsea.brunner@wku.edu), [7](mweisberg@kbcc.cuny.edu).

Introduction: Carbonaceous chondrites result from the accretion of solids formed in the protoplanetary disk (a.k.a., solar nebula). The principal solid components (clasts) are: Ca-, Al-rich inclusions (CAIs [1]), chondrules of various textural and chemical subtypes, amoeboid olivine aggregates (AOAs [2-4]), lithic fragments (dark inclusions) of primitive meteoritic material, and isolated olivine grains.

The CV chondrites are distinguished as a group by texture (clast size [5], chondrule/matrix ratio [6]) and enrichment in refractory lithophiles [6]. They occur in reduced and oxidized subtypes [7-8]. The variations between chondrite groups are thought to represent localized heterogeneity of the nebular environment in which chondrites formed [9]. Here, we report much larger differences in clast/matrix ratios between reduced and oxidized subtypes than [7], and we infer that ices accreted with matrix were the oxidizing agent in CV chondrites.

It follows that quantitative knowledge of the size distributions and relative abundances of clasts in CV chondrites are required for constraining and testing models for the accretion of meteorite parent bodies. For example, the size sorting observed in chondrite classes may result from aerodynamic sorting of clasts in turbulent eddies [10], or during sedimentation or radial drift [11]. The chondrule type abundances in CV chondrites are well known only for Allende [16]. Models of shock heating predict the abundances of chondrule clasts of various types produced for assumed initial parameters [13]. The accretion of chondrule precursor material is, presumably, reflected in the size and chemical type of chondrules found in chondrites.

Furthermore, the relative abundances of clasts, and their bulk chemical characteristics, determine the bulk composition of every class of chondrite. The marked similarity of these bulk compositions is a first order phenomenon in meteoritics [14-16]. The relative proportions of clasts of different bulk chemical composition (e.g., CAIs vs. chondrules), and clast/matrix ratios, are fundamental data in addressing the formation conditions of parent bodies. Thus we are strongly motivated to apply modern methods to aggregate clast analysis [17], building on the pioneering work of [7].

Methods: Polished thin sections (PTS) of Bali, Mokoia, Vigarano, Leoville, Nova-002 and Allende, and thick sections (PS) and random cut slabs of Allende were mapped in major elements at 13 (slabs), and 4 to 9 μm/pixel resolution (sections) [17] (Table 1). Element, BSE, and RGB composite map mosaics were superposed to allow masking, manual outlining of inclusions, and determination of inclusion type [17]. The superposition of multiple elemental and composite maps, costly in computer resources, is invaluable in performing this work.

Hand-drawn inclusion outlines - the critical step, and determination of inclusion type, have been checked by at least two authors independently for all samples. Types of chondrules (PP, PO, POP, BO, RP), CAIs (CTA, FTA, B, misc.) and other components were grayscale-coded, and the numbers of pixels representing inclusions of each type were counted [17]. The original EMP pixel resolution was preserved throughout. Table 1 records the analyzed and counted area of each meteorite, in pixels and cm^2.

Results: Clast abundances for five CV chondrites are presented in Table 1, with a comparison to earlier work [7], and calculated ratios of clasts (CAI + AOA + chondrule) to matrix (matrix + isolated olivine + dark inclusions) for both data sets. The wide diversity in clast/matrix ratios in our data is illustrated in Fig. 1, with the Allende-type oxidized CV below, and the reduced CV above. Nova 002 is highly weathered, and not yet classified for subtype. We intend to analyze more sections of each CV, however, small Allende sections yielded results consistent with analyses of large slabs.

Size distributions of chondrules, AOAs, and CAIs (combined as 'clasts') were determined separately from the outlined images of each chondrite. Table 1 presents log-normal radius data for *n* clasts in each section, where r are the radii of circles with same areas as the *n* clasts. For Allende, size data is for a single 16 cm^2 slab area imaged at 13 μm/pxl (AL-4884-s2B). The low skewness of the distribution results from the large number of clasts.

Reduced vs. oxidized CV: An unexpected result, not anticipated by [7], is the large difference in clast/matrix ratio between the oxidized and reduced subgroups of CV chondrites. In [17], we remarked on the high abundance of matrix in Allende. Here we confirm a similar abundance in Mokoia. Our clast to ma-

trix ratios for the oxidized subgroup lends support to the idea that ices are transported into chondrite parent bodies with matrix [18, and references therein]. Thus the alteration in the oxidized CVs may be attributed to the presence of more ice-bearing matrix than accreted into the reduced CVs.

Table 1: Abundances of clasts in CV chondrites measured here, compared to those reported by [7]. Area (pixels) reports integral number of pixels actually counted; 'stdevp' is 1σ.

meteorite	Allende	Mokoia	Nova002	Vigarano	Leoville		
type	CV3.2-oxA	CV3-oxA	CV3	CV3.0-red	CV3.0-red		
sample source	AMNH	AMNH	AMNH	AMNH	USNM		
sample number	multiple	3906-4	4826-2	2226-4	3535-1		
micron/pixel	4 to 13	9	7	7	10		
Area (pixels)	88,863,999	1,035,734	1,923,983	848,249	1,639,210		
Area (cm^2)	120.595	0.839	0.943	0.416	1.639	avg	stdevp
matrix	61.47	54.18	36.41	33.33	31.50	43.38	12.12
CAI	4.30	4.91	0.76	2.40	1.83	2.84	1.54
AOA	3.05	2.00	3.87	1.78	4.02	2.94	0.92
chondrule	30.95	38.08	56.95	62.40	62.44	50.16	13.13
met/sul	0.18	0.79	0.34	0.10	0.21	0.32	0.25
unknown	0.1	0.0	1.7	0.0	0.0	0.35	0.66
clasts/matrix	0.62	0.82	1.68	1.99	2.15	1.45	0.62
n clasts	1096	185	172	462	265	436	346
mean, ln(r)	5.6147	4.7789	4.9667	3.7648	5.1084	4.85	0.61
variance, ln(r)	0.3493	0.9809	1.1734	0.9420	1.0440	0.90	0.29
skewness, ln(r)	0.012	-0.573	-0.478	0.599	-0.390	-0.17	0.43
ref. [7] :	Allende	Mokoia	n.a.	Vigarano	Leoville	avg	stdevp
points counted	1572	1510		1594	1705	1595	
matrix	41.3	43.4		36.6	36.2	39.38	3.07
CAI	9.4	3.5		5.3	6.6	6.20	2.15
AOA	3.2	2.7		5.4	1.3	3.15	1.47
chondrule	43	46.9		48.9	51.4	47.55	3.07
opaques	3.1	3.5		3.0	4.5	3.53	0.59
clasts/matrix	1.25	1.13		1.51	1.46	1.34	0.15

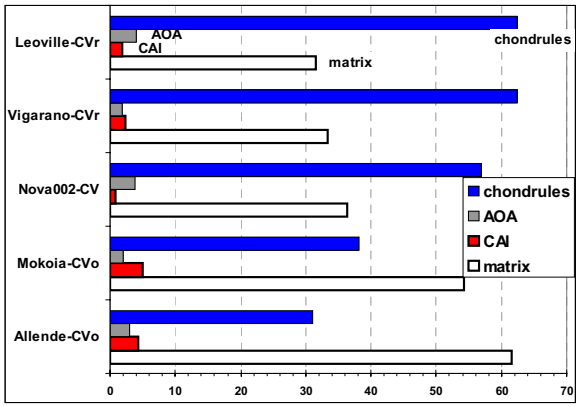

Fig. 1: Abundances of major components in CV chondrites. Statistics are most robust for Allende.

Astrophysical Implications: Earlier workers have quantified the radii and densities (r and ρ) of small numbers of chondrules separated from chondrites [19], or quantified clast size and density by tomography [20]. These are the vital parameters for dynamical model calculations [10,11]. Our results address this need, and we have in hand 3D microtomography data to supplement 2D surface investigations.

Future Work: We are writing software to use element x-ray intensity maps, combined with outlines of clasts, for qualitative, pixel-by-pixel assessment of the relative abundances of major elements between individual clasts. This will allow us to measure: the abundance of metal/sulfide subgrains inside chondrules; chondrule pyroxene/olivine ratios; the mean FeO content of silicates to identify Type I and II chondrules [7]; the Ca/Al ratio in each CAI. We should, then, also be able to estimate clast densities (ρ).

Distinct igneous layers or accretionary rims surround many clasts, evidence of the origin and histories of the clasts themselves. Although there have been anecdotal reports of correlations between clast type, clast size, and rim thickness, there is no strong quantitative evidence regarding such relationships. With consistent criteria, rim thicknesses could be quantified.

Conclusions: There is a clear dichotomy in clast/matrix ratio in CV chondrites. The oxidized subgroup has nearly twice the matrix abundance, and nearly half the chondrule abundance, of the reduced subgroup. Matrix abundance and oxidative alteration are correlated. Image analysis, with careful, deliberate application of human expertise, can provide the statistical power and quantitative constraints necessary to address major problems of chondrule and CAI origin and accretion into protoplanetary bodies [21, 22].

References: [1] MacPherson G.J. et al. (2005) In *Chondrites and the Protoplanetary Disk* (eds. Krot A.N. et al.) p.3-242. [2] Grossman L. & Steele I.M. (1976) *GCA, 40,* 149-155. [3] Weisberg M.K. et al. (2004) *MPS, 39,* 1741-1753. [4] Krot A.N. et al. (2004) *Chemie der Erde, 64,* 185-239. [5] Van Schmus W.R. (1969) *Earth-Science Reviews, 5,* 145-184. [6] Van Schmus W.R. & Hayes J.M. (1974) *GCA, 38,* 47-64. [7] McSween H.Y. Jr. (1977) *GCA, 41, 1777-1790.* [8] Weisberg M.K., McCoy T. J., Krot A.N. (2006) *MESS2* p. 19-52. [9] Brearley A. & Jones R. (1998) In *Planetary Materials* (J. J. Papike, ed.), pp 3-1 - 3-398. [10] Cuzzi J.N. & Weidenschilling S.J. (2005) *MESS2* p. 353-381. [11] Brauer F. et al. (2007) *Astronomy & Astrophysics, 469,* 1169-1182. [12] Grossman J.N. (1988) In *Meteorites and the Early Solar System* (eds. J. F. Kerridge & M.S. Matthews), U. Arizona Press, ch. 9.3 [13] Desch S.J. & Connolly H.C. Jr. (2002) *MPS, 37,* 183-207. [14] Palme H. et al. (1992) *LPS XXIII, 1021-1022*. [15] Bland P.A. et al. (2005) *Proc. National Acad. Sci., 102, 13755-13760.* [16] Palme H. & Pack A. (2008) *LPS XXXIX* #1821. [17] Ebel D.S., C.E. Brunner, M.K. Weisberg (2008) *LPS XXXIX* #2121. [18] Zanda B. et al. (2008) *LPS XXXIX* #1532. [19] Paque J. & Cuzzi J.N. (1997) *LPS XXVIII,* p.1071–1072. [20] Kuebler K.E. et al. (1999) *Icarus, 141,* 96-106. [21] Mayne R.G. et al. (2009) *GCA, in press.* http://dx.doi.org/10.1016/j.gca.2008.10.035 [22] Brunner C.E. et al. (2008) *MPS Suppl., 43*, A28.

MESS2 = Meteorites and the Early Solar System II, (D. Lauretta et al., eds.) U.Arizona, Tucson; *GCA = Geochimica et Cosmochimica Acta*; *MPS = Meteoritics and Planetary Science*; *LPS = Lunar & Planetary Science*, LPI.

Acknowledgments: Research was supported by U.S. N.A.S.A. grants NANG06GD89G (DSE) and NANG06GG446 (MKW). The AMNH Physical Sciences REU Program (NSF #AST-055258) supported C.E.B. (2007) and K.L. (2008). This research has made use of NASA's Astrophysics Data System Bibliographic Services.